# A Protocol to Evaluate One Electron Redox Potential for Iron Complexes

Hyungjun Kim,[a] Joungwon Park,[b] and Yoon Sup Lee *[a]

Density functional theory calculation has been performed to calculate the redox potential and the correct ground spin state of iron complexes in acetonitrile. Widely used B3LYP functional is applied with the spin state corrected basis sets. The newly developed protocol for the set of 21 iron complexes is to optimize the structure at the level of the B3LYP/6-31G* and to calculate the single point electronic energy with the same functional and the modified basis sets s6-31G* for the iron atom and 6-31+G* for other ligand atoms. The solvation energy is considered through the polarized continuum model and the cavity creation energy is included for the accurate spin state description. Modifying the cavity size by employing the different scaling factor according to the mean absolute value of the natural population analysis charge (MA-NPA) is introduced. The molecule with the large MA-NPA requires the cavity size smaller than the less polar one. This protocol gives only 1 wrong ground spin state among the 18 iron complexes for which experimental data are known. For the open circuit voltage (OCV) calculation, our protocol performs well yielding the mean absolute error of 0.112 V for the test set. The close correlation between the calculated and the experimental OCV are obtained. © 2013 Wiley Periodicals, Inc.

DOI: 10.1002/jcc.23380

## Introduction

The iron complexes are widely used as an active material of the redox flow battery. This type of the battery has high-storage capacity. The coupled active materials are continuously oxidized and reduced to produce electricity. One of the necessary conditions for being the efficient material is high open circuit voltage (OCV). OCV is often used to refer to the reduction potential in the battery research field. Designing of new candidates and investigating the origin of high redox potential can be an objective of quantum computational chemistry. The accurate potential difference of each redox couple is required for the prediction of OCV. There have been several studies regarding the prediction of the redox potential of transition metal complexes and small organic compounds.[1–16] Due to the large number of atoms, high level *ab initio* approaches are rarely found. Density functional theory (DFT) methods, which can handle the large compound, are widely used and show the robustness in many fields involved metal complexes such as the catalyst and the battery. Despite the popularity, DFT approaches have some limitation in dealing with the transition metal complexes in battery. The first one is related to predicting the correct ground spin state because the OCV calculation based on the wrong ground spin state is not so meaningful. Whether the spin state is high or low depends on the energy gap of metal *d*-orbital. In many previous works, the results strongly depend on the type of the DFT functional.[17–21] The pure functional prefers the low spin state, but calculations based upon the hybrid functionals such as B3LYP and PBE0 show that the high spin state is more stable due to the inclusion of the Hartree-Fock (HF) exchange. Focusing on the high percentage of the HF exchange in the B3LYP leads Reiher and coworkers to lower its amount from 20 to 15% for the correct spin state calculations and named the modified method as B3LYP*.[22] The recent study, however, shows that even the B3LYP* fails to reproduce the experimental ground spin state for some iron complexes. The even lower 12% of the HF exchange with the empirical term can fix this problem.[13]

Other authors point out that the failure of the prediction for the spin state might originates from incomplete basis sets.[23] The recent articles also criticized the use of the effective core potential (ECP) for the metal and do not recommend to use the Gaussian type orbital basis sets because of its slower convergence than the Slater type basis sets.[23] The spin-state corrected basis sets, which are the Pople's basis sets augmented by one diffuse *d*-orbital function, are newly constructed and used to estimate the spin state of 13 transition metal complexes successfully.[24] The name of the modified basis set is denoted as the original basis set name appended by the prefix "s" in front.

The second problem is the accuracy of the electric potential difference between the reduced and the oxidized ones. Despite many attempts, DFT still offers a limited accuracy. There have been attempts to solve the problem by including the empirical parameter or shifting calculated values to induce the good correlation with the experimental data.[2,13] It is

[a] *H. Kim, Y. S. Lee*
*Department of Chemistry, KAIST, Daejeon 305-701, Korea*
[b] *J. Park*
*Battery Group, Energy Lab, Samsung Advanced Institute of Technology, Samsung Electronics, Giheung-gu, Yongin-si, Gyeonggi-do 446-712, Korea*
*E-mail: yslee@kaist.edu*

Contract grant sponsor: Ministry of Knowledge Economy, Republic of Korea; contract grant number: 2011201010007A; Contract grant sponsor: NRF; contract grant number: 2007-0056095

unsatisfactory that the deviation gets larger for highly charged species, and the deviation is not systematic.

Because the active materials are immersed in solvents, the molecular environment is different from the gas state. The explicit solvent calculation is almost impossible for the quantum mechanical calculation due to the large number of solvent molecules. Herein, the one of the implicit solvation models, the polarizable continuum model (PCM)[25] that treats solvent molecules as the reaction field, is used. The solute molecule is immersed in the vacuum cavity space and molecular charge fitted to reproduce the electrostatic potential is spread on the surface of cavity. The cavity volume size is determined using interlocking of the individual solute atomic radii which are proportional to the atomic van der Waals (vdW) radii. The scaling factor *f*, which multiplies the vdW radii, is initially set as 1.2.[26] Gaussian09[27] provides the vdW radii from the universal force field (UFF) calculation and *f* of 1.1.

In this article, we examined the optimal protocol for the prediction of the accurate redox potential and the correct ground spin state simultaneously for the $[Fe(Bpy)_3]^{3+/2+}$ (Bpy=2,2′-bipyridinyl) in terms of the basis sets and the solvation energy. We apply this protocol to the set of the iron complexes for which OCV values and ground spin state are known. The effect of the cavity creation energy and the energy variance according to the scaling factor are inspected.

## Computational Details

### Redox potentials calculation

All the calculations are carried out using Gaussian09 package. The thermodynamic cycle in Figure 1 is used to calculate the redox potential.

The redox potential ($E^0$) can be evaluated using the following equation.

$$E^0 = \frac{\Delta G}{nF} = -\frac{\Delta G_s - \Delta G_{SHE}}{nF}$$

where *n* is the mole number of electron and *F* is the Faraday constant equal to 23.06 kcal/mol V. In Figure 1 and other places, 'Ox' and 'Red' mean the oxidized and reduced complex, respectively. The gas state and solution state are presented using "g" and "s" in the parenthesis. The Gibbs free energy difference in the solution $\Delta G_s$ can be divided into the Gibbs free energy difference in the gas phase $\Delta G_g$ and the solvation energy difference $(\Delta\Delta G_{sol} = \Delta G_{sol,red} - \Delta G_{sol,ox})$.$\Delta G_{sol,red}$ and $\Delta G_{sol,ox}$ represent the solvation energy of reduced and oxidized form. The Gibbs free energy in the gas phase $\Delta G_g$ is the sum of the electronic energy ($E_0$), the zero point energy (ZPE) and the thermal correction. The standard hydrogen electrode reduction potential reported by many groups ranges from 4.2 to 4.73 V. We choose 4.44 V recommended by IUPAC.[28]

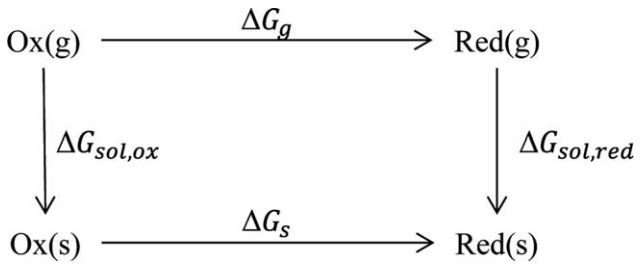


**Figure 1**. The thermodynamic cycle used to describe the redox potential.

### Geometry optimization and frequency, single point energy calculation

In the geometry optimization step, the B3LYP functional and the variety of basis sets (6-31G, 6-31G*, 6-311G, 6-311G*, and s6-31G*[24] were tested. The geometry optimization was performed using B3LYP and U-B3LYP for singlet and high multiplicity complex, respectively. The spin contamination of the complex with high multiplicity is not significant. The B3LYP functional is selected due to its known reasonable performance for the property of transition metal complexes and the comparison here with other DFT functionals confirms this as shown later.[2,29,30] Frequency calculation is followed at the same level of theory. The ZPE and the thermal correction at room temperature are derived from the frequency calculation. The electronic energy calculation, which is relatively less expensive than the frequency calculation, is done with the larger basis sets at this fixed geometry.

### Solvation energy

The solvation energy is taken into consideration by PCM. The solvation energy is decomposed into four terms, electrostatic energy (Elec), dispersion energy (Disp), cavity creation energy (Cav), and repulsion energy (Rep). Considering that the spin state energy gap is very small, it is possible that contributions of other terms are not negligible. There are previous reports that the different scaling factor should be used according to the system to be described.[31,32] The charged molecule needs to be computed with the scaling factor *f* of 1.10 or 1.15, smaller than the default value of 1.2, in the past.[33,34] As the appropriate scaling factor for highly charged iron complexes has not been reported yet, we tested the three scaling factors $f = 1.0$, 1.1, and 1.2. The change of solvation energy and redox property is investigated to arrive at optimal values of *f*. We are not trying to minimize the calculation error for each redox couple, but to show a general way to improve the performance of PCM for the calculation of highly charged metal complexes.

## Result and Discussion

### Geometry of the ground state

It is necessary to reproduce the experimental structure to obtain the accurate energy. The geometry of the $[Fe(Bpy)_3]^{2+}$ is optimized with the B3LYP functional using the various basis sets. The experimental structure data have been reported.[35] The crystal structure obtained in the form of $[Fe(Bpy)_3](PF_6)_2$ was published.[36] The bond distance between the metal atom and the nitrogen donor atoms is compared carefully. This

distance is highly related to the spin state splitting energy.[19] The bond distances within the ligand are also important as the most solvation energy comes from the surface of the ligand. The selected eight bond distances are compared in Supporting Information Table S1 and the corresponding atomic symbol and numbering are indicated in Supporting Information Figure S1. Basis sets 6-31G* for all atoms are chosen to optimize the ground state geometry considering mean absolute error (MAE) of the bond distance.

### Ground spin state prediction

The prediction of the ground spin state is conducted by comparing the Gibbs free energy of the reduced and oxidized form. The ZPE and the thermal correction are calculated at the same level of theory as that applied to the geometry optimization as the vibrational frequencies are meaningful when calculated for the optimized structures. The electronic energy is refined by the single point energy calculation using more extensive basis sets. For $[Fe(Bpy)_3]^{2+}$, the spin splitting energy gap considering only the electronic energy ($\Delta E^{el.}_{HS\text{-}LS}$) without ZPE and the thermal correction has been reported as 3500∼6000 $cm^{-1}$ which is derived from the spin relaxation dynamics at low temperature. The $\Delta E^{el.}_{HS\text{-}LS}$ value and the prediction of the ground state are tabulated in Supporting Information Table S2.

From the results summarized in Supporting Information Table S2, we conclude that 6-31+G for the ligand and s6-31G* or 6-31+G* for core metal is the optimal combination to be consistent with the experiment for the ground spin state property.

### Redox potentials

The objective of this study is to calculate OCV consistently close to the experimental values based on the correct ground spin state predictions. The experimentally known OCV for the $[Fe(Bpy)_3]^{3+/2+}$ couple in acetonitrile solvents is approximately 1.302 V. The same combination of the basis sets used in the spin calculation is applied to get the insight of the basis sets effect on OCV. Supporting Information Table S3 summarizes the OCV results.

The combination of the s6-31G* basis set for the metal atom and the 6-31+G* basis sets for light atoms seems to be optimal among those considered here.

In order to justify further the choice of the B3LYP functional, the performance of B3LYP is compared with other four DFT functionals, BLYP, OPBE, M06-2X, and PBE0, which are widely used in calculation of transition metal complexes. The optimized Fe—N bond distance and the reduction potential of $[Fe(bpy)_3]^{3+/2+}$ are calculated using s6-31G* for the iron atom and 6-31+G* for other light atoms. The M06-2X functional predicts the Fe(III) as the high spin of a sextet and its OCV result is not considered. The bond length of a singlet Fe(II) is predicted to be 1.984, 1.941, 2.040, 1.973, 1.997 Å for BLYP, OPBE, M06-2X, PBE0, and B3LYP, respectively, and experimental data is 1.967 Å. Even though B3LYP shows some error in describing the Fe—N distance, its deviation 0.03 Å is within the range of an accurate functional. Hybrid functionals seem to overestimate the bond length. GGA functionals OPBE shows shorter bond length, while other GGA functional BLYP predicts longer than experimental data. The reduction potential is underestimated in all cases compared with the experimental value 1.302 V in acetonitrile. The difference between experimental data and the B3LYP result 1.170 V is 0.13 V, which is quite similar to OPBE's 1.182 V. BLYP and PBE0 predict 1.030 and 1.085 V, respectively, with errors somewhat larger than B3LYP.

### Cavity creation energy

All the solvation calculations were performed using Gaussian09 with the default parameters. Most of the solvation energy comes from the electrostatic energy, but there is a non-negligible contribution from other terms. Table 1 lists the Cav, Disp, and Rep energy contribution in the Fe(II) and the Fe(III) complexes.

**Table 1.** The energy change from the inclusion of the other effects ( in kcal/mol, LS stands for low spin and HS for high spin).

| | LS(+2) | HS(+2) | LS(+3) |
|---|---|---|---|
| Cav | 54.7 | 58.2 | 54.9 |
| Disp | −26.1 | −26.7 | −26.1 |
| Rep | 1.5 | 1.6 | 1.5 |

The solvent–solute repulsion interaction and the dispersion energy are quite small for all the complexes, and the difference between the low and the high spin states of the same charge is negligible. The charge distribution is different between the reduced form and the oxidized form, but the vdW interaction which is mostly determined by the type of atom is not much different. The cavity creation energy, which is required to make a vacuum space for the solute molecule in solvent, take a quite large portion, roughly 20% of the solvation energy. The Fe—N bond stretches during the transition from the singlet to the quintet states, and causes the volume enlargement. Creating a larger volume cavity requires more energy. The difference of cavity creation energy between the singlet and the quintet state complexes is obtained as 3.5 kcal/mol, and this somewhat relieve the deviation caused by the favoring of the high spin states in DFT calculations with hybrid functionals. As the Fe—N distance is reduced by only 0.002 Å during the oxidation process, the cavity creation contribution is negligible in the OCV calculation.

### Scaling factor

The cavity size for the different solute molecule cannot be recommended universally because the actual size of ions in solution should change according to molecular chemical environment. The UFF radii already taking the hybridization state into accounts still lack the atomic partial charge information. We find that the variation of cavity size by adjusting the scaling factor can improve the performance of DFT on the OCV calculation, since the amount of the charge interaction

**Table 2.** The OCV and the spin state property variation according to the scaling factor with and without the cavity creation energy (The OCV is written in V and the spin state property is in $cm^{-1}$).

| | OCV | | $\Delta E^{el}_{HS-LS}$ | | $\Delta G_{HS-LS}$ | |
|---|---|---|---|---|---|---|
| | w/o Cav | w/ Cav | w/o Cav | w/ Cav | w/o Cav | w/ Cav |
| 1.0 | 0.89 | 0.88 | 2832 | 4040 | 346 | 1555 |
| 1.1 | 1.17 | 1.17 | 3177 | 4386 | 691 | 1900 |
| 1.2 | 1.40 | 1.39 | 3234 | 4443 | 748 | 1957 |

can be modified by controlling the scaling factor. Table 2 describes the OCV and the spin property variations according to the scaling factor with and without the cavity creation energy.

The calculated OCV utilizing the smaller cavity size is 0.89 V which is reduced by 0.28 V from the one using the default parameters. Conversely, the enlarged cavity size increases OCV to 1.40 V which is in better agreement with the experimental value 1.302 V than other two results. The energy change of the +3 ion 13.9 kcal/mol due to the increase of $f$ is bigger than that of the +2 ion 7.4 kcal/mol. During the change from $f = 1.1$ to $f = 1.2$, 10.4 kcal/mol for the +3 ion and 5.2 kcal/mol for the +2 ion are obtained. The energy gap becomes larger as the larger scaling factor is selected. As the more concentrated charge is spread on the surface of cavity, the charge interaction becomes more sensitive to the cavity size change. The complex, for which the calculated OCV with the unmodified $f$ is lower than the experimental data, shows improvement upon using $f = 1.2$. The OCV value increases from 1.17 to 1.40 V. We assume that the complex bearing highly charged exposed part should be described using smaller cavity based on the intuition that solvent molecules, in average, may get closer to the highly charged one compared with the less charged one. The complex with smaller amount of charges on surface should be modeled using larger cavity.

### Application to the test set

The protocol developed is applied to the test set. The test set molecules are selected from Ref. [13] and described in Figure 2.

The redox potentials of all 21 compounds have been reported in Ref. [13], but the ground spin state has been confirmed experimentally only for 18 molecules. All of the test set molecules undergoes the reduction from Fe(III) to Fe(II), except [Fe(CyclamAc)($N_3$)] which is reduced from Fe(IV) to Fe(III) and Fe(II). According to the octahedral ligand filed splitting, the Fe(II) complex takes a singlet as the low spin state when all the *d*-orbital electrons are distributed in the three $t_{2g}$ orbitals and a quintet as the high spin state when four electrons are in the three $t_{2g}$ and two in the two $e_g$ orbitals. The Fe(III) complex would be a doublet as the low spin state by distributing five electrons in the three $t_{2g}$ orbitals with two doubly occupied and one singly occupied orbitals. A sextet state as the high spin state is obtained by putting three electrons in the three $t_{2g}$ and two electrons in the two $e_g$ orbitals. Meanwhile *d*-orbitals of the complexes having four ligands would split according to the tetrahedral ligand field splitting. A triplet and a quintet spin state would be taken by Fe(II). For the Fe(III) case, possible spin states are same as those of the octahedral one. The result of the spin state prediction is shown in Table 3.

Estimation of the ground spin state with B3LYP/LACVP**[13] fails in reproducing the experimental ground spin state for nine cases due to the over-stabilization of the high spin complex. We tested all electron basis sets of similar size 6-31G* for the metal atoms to avoid the errors due to the use of ECPs. Complexes with the $Pyr_2Py$, the $TacnPy_2$ and the $N_4Py$ ligands now have the experimental ground spin states partly owing to the inclusion of core electrons, but still six molecules are in the wrong ground spin state. The augmenting 6-31G* with diffuse functions on the ligand molecules and the use of the spin state corrected basis sets further remove two wrong spin state predictions. The energy gains differ depending on the molecular charge and the ligand character. The low spin state complexes usually stabilized more by ~2 kcal/mol, and this contributes to alleviate B3LYP's favor for the high spin state. The augmented diffused function on the metal atom plays a significant role probably because the diffuse function helps to describe the unpaired electrons occupying the *d*-orbital. There still remain four problematic molecules. The volume occupied by the solute molecules is quite different between the low spin and the high spin complexes. For example, singlet and quintet $[Fe(bpy)_3]^{2+}$ have volumes of 636.71 and 657.29 $Å^3$, respectively, according to the estimate by the GePol code[37–39] of Gaussian09. The amount of energy to remove the reaction field of acetonitrile solvent (dielectric constant value is 35.69) are 54.7 and 58.19 kcal/mol for the low and the high spin states, respectively, resulting in additional 3 kcal/mol destabilization of the high spin state. Inclusion of cavity creation energy fixes three of four complexes and only one is left as different from the experimental ground spin state. We also examined the molecular orbitals obtained for the complex ions and confirmed that the electrons are mainly distributed in the *d*-orbitals of the Fe atom for high-lying occupied, fully or partially, orbitals. (Supporting Information Fig. S5) Volume expansion during the transition from the singlet to the quintet state is confirmed by the Fe—N bond elongation of 0.16–0.2 Å[40,41]. The energy changes due to the cavity size difference between the singlet and the quintet states are ranging 1.5–3.5 kcal/mol for all other iron complexes.

### Redox potential

The deviation from the experimental findings would occur in the solvation energy calculation process assuming that the gas phase energy calculation is accurate enough. The PCM is successfully applied in property calculations of many small molecules. We focus that the highly charged solute is the source of the problem, not the PCM way of treating solvent molecules. The study regarding the cavity size for the highly charged system has not been studied yet. Therefore, we assume that most if not all solvation energy error can be cancelled by adjusting the scaling factor based on the charge environment

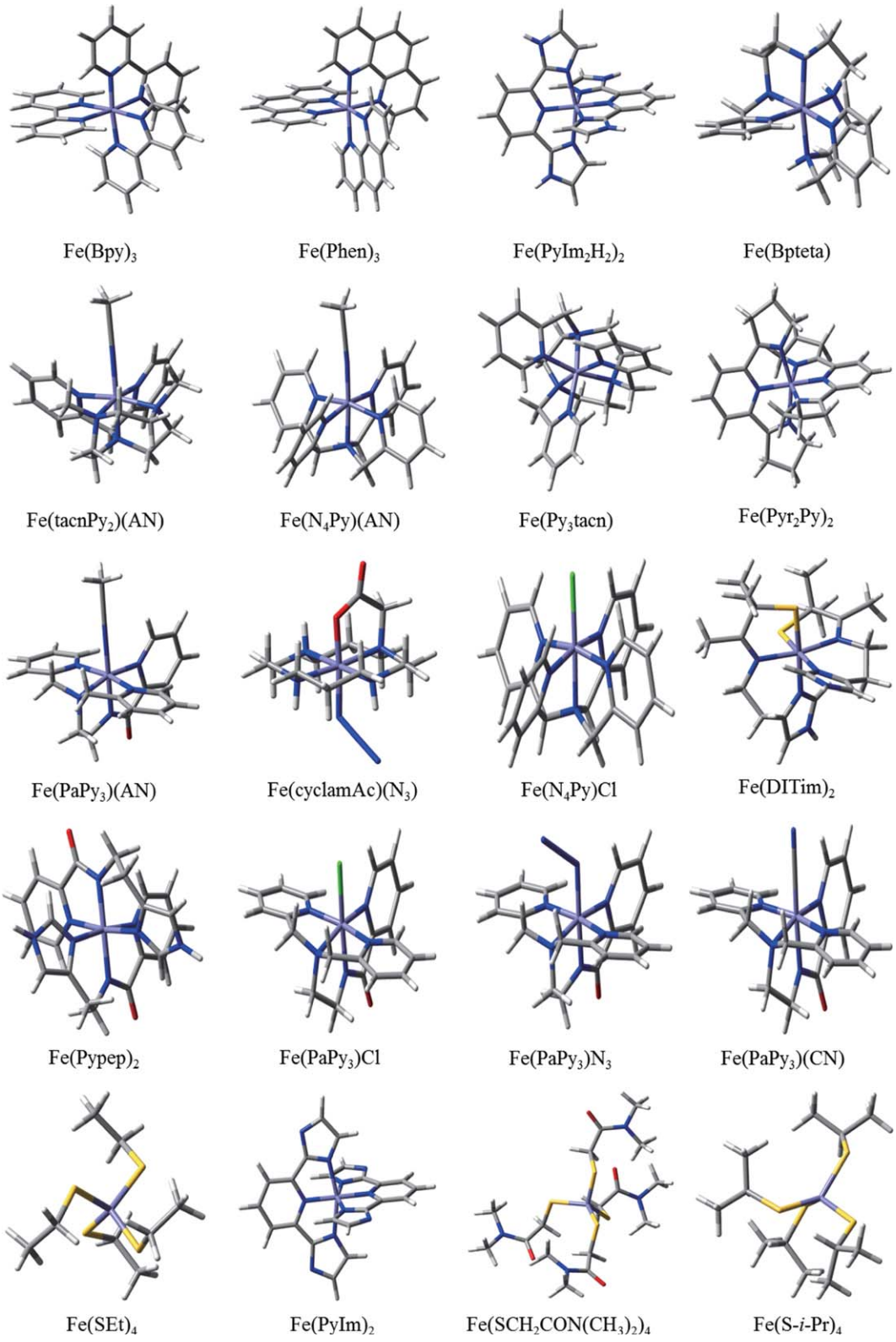


**Figure 2.** The test set of iron complexes (The short name is chosen from Ref. 13).

of each molecular ion. Table 4 lists the calculated and the experimental OCV of the test set.

We notice that most calculated OCV increase as the scaling factor increases, but some redox couples exhibit the opposite behavior. The energy variance according to the scaling factor change implies that the molecule containing more charge would be more sensitive to the solute molecule volume. The slope of the energy with respect to the scale factor increases in the order of 0, +1, +2, and +3 for the ionic charge. This concept can also be applied for the negatively charged molecule. The gradient for the −1 ion is less steep than the one for the −2 ion and the larger OCV can be obtained by shrinking the molecular cavity volume. There are some exceptions like $[Fe(DITim)_2]^{1+/0}$ and $[Fe(Papy_3)(Cl)]^{1+/0}$ whose OCV become smaller as the size of cavity increases. These complexes undergo the redox reaction from the low spin state of the oxidized form to the high spin state of the reduced form, and the high spin complex has larger partial charges than the low spin counterpart.

We performed the natural population analysis (NPA) calculation at the level of the single point calculation to validate the assumption made in the scaling factor part. The value of the mean absolute of the NPA charge in highly charged exposed part (MA-NPA) is utilized to judge the degree of charge concentration and separation. The amount of charge commonly obtained for exposed aromatic carbon and hydrogen atoms is at most 0.3 in absolute scale in the molecules of our test set. Considering this charge environment as the norm, only the more highly charged exposed atoms are included to evaluate MA-NPA.

**Table 3.** The prediction of the ground spin state for iron complexes with the different basis sets combinations.

| Spin state (Fe basis sets, light atoms basis sets) | B3LYP LACVP 6-31G* | B3LYP 6-31G* 6-31G* | B3LYP s6-31G* 6-31+G* | B3LYP s6-31G* 6-31+G* w/ cav | Exp |
|---|---|---|---|---|---|
| $[Fe(Bpy)_3]^{2+}$ | 2 | 0 | 0 | 0 | 0 |
| $[Fe(Phen)_3]^{2+}$ | 2 | 2 | 2 | 0 | 0 |
| $[Fe(PyIm_2H_2)_2]^{2+}$ | 2 | 2 | 2 | 2 | Spin-crossover |
| $[Fe(PyIm_2)_2]^{1-}$ | 1/2 | 1/2 | 1/2 | 1/2 | 1/2 |
| $[Fe(Bpteta)]^{2+}$ | 2 | 2 | 2 | 0 | 0 |
| $[Fe(DITim)_2]^{1+}$ | 1/2 | 1/2 | 1/2 | 1/2 | 1/2 |
| $[Fe(Pypep)_2]^{1+}$ | 1/2 | 5/2 | 1/2 | 1/2 | 1/2 |
| $[Fe(PaPy_3)(AN)]^{2+}$ | 1/2 | 1/2 | 1/2 | 1/2 | 1/2 |
| $[Fe(PaPy_3)Cl]^{1+}$ | 5/2 | 1/2 | 1/2 | 1/2 | 1/2 |
| $[Fe(PaPy_3)(N_3)]^{1+}$ | 5/2 | 5/2 | 1/2 | 1/2 | 1/2 |
| $[Fe(PaPy_3)(CN)]^{1+}$ | 1/2 | 1/2 | 1/2 | 1/2 | 1/2 |
| $[Fe(CyclamAc)(N_3)]^{1+}$ | 1/2 | 1/2 | 1/2 | 1/2 | 1/2 |
| $[Fe(CyclamAc)(N_3)]^{0}$ | 2 | 2 | 2 | 2 | 0 |
| $[Fe(TacnPy_2)(AN)]^{2+}$ | 2 | 0 | 0 | 0 | 0 |
| $[Fe(N_4Py)Cl]^{1+}$ | 2 | 2 | 2 | 2 | 2 |
| $[Fe(N_4Py)(AN)]^{2+}$ | 2 | 0 | 0 | 0 | 0 |
| $[Fe(Py_3tacn)]^{2+}$ | 2 | 2 | 2 | 0 | 0 |
| $[Fe(PyrPy)_2]^{2+}$ | 2 | 0 | 0 | 0 | 0 |
| The number of molecules in wrong spin state | 10 | 6 | 4 | 1 | – |

Among eight 3+/2+ redox couples, $[Fe(Bpy)_3]^{2+}$, $[Fe(Phen)_3]^{2+}$, and $[Fe(Pyr_2Py)_2]^{2+}$ have exposed hydrogen atoms with charge of +0.27 which is considered as usual for aromatic carbon and hydrogen atoms. The predicted OCVs show somewhat improved result 1.398, 1.380, and 1.381V, respectively, when using $f = 1.2$. For the complexes with Bpy and Phen ligand, more improved OCV results of 1.29 and 1.277 V, respectively, can be obtained with $f = 1.15$. Remaining five complexes have larger MA-NPA than the preceding ones. $[Fe(Bpteta)]^{2+}$ has highly charged four hydrogen atoms which are bonded to the $sp^3$ nitrogen atom, and their average charge is 0.442. $[Fe(PyIm_2H_2)_2]^{2+}$ also has highly positive hydrogen atoms whose MA-NPA is 0.497. $[Fe(Py_3tacn)]^{2+}$ has three $sp^3$ nitrogen atoms bearing −0.485. The complexes ligated with an acetonitrile, such as $[Fe(tacnPy_2)(AN)]^{2+}$ and $[Fe(N_4Py)(AN)]^{2+}$, have concentrated charge on the acetonitrile molecule. MA-NPAs of these molecules are 0.417 and 0.416, respectively. All five molecules are well described using $f = 1.1$. A more remarkable progress on the prediction can be made for $[Fe(tacnPy_2)(AN)]^{2+}$, $[Fe(N_4Py)(AN)]^{2+}$, and $[Fe(PyIm_2H_2)_2]^{2+}$ by shrinking the cavity size. We observe that those complexes have highly charged atoms such as the methyl group carbon atom of acetonitrile bearing −0.797 and the exposed $sp^3$ nitrogen atom bearing −0.511. The scaling factor $f = 1.05$ is better due to the fact that these sites can interact with solvent molecules more strongly. The predicted results are 1.091, 1.340, and 0.894 V, respectively. MAE of the 3+/2+ redox couples 0.114 V drops to 0.047 V when using the optimal scaling factor. For the 3+/2+ couples, the complex whose MA-NPA is smaller than 0.3 is well described using $f = 1.15$. For the molecule with the natural charge larger than 0.3, the default scaling factor shows good performance. Scaling factor is varied by 0.05 to find the optimal value for the complex.

**Table 4.** The calculated OCV for iron complexes with different scaling factors. (in V, OCV calculated with the optimal scaling factor is italic-typed.)

| OCV | 1.0 | 1.05 | 1.1 | 1.15 | 1.2 | Exp |
|---|---|---|---|---|---|---|
| 3+/2+ redox couple | | | | | | |
| $[Fe(Bpy)_3]^{3+/2+}$ | 0.891 | – | 1.172 | *1.290* | 1.398 | 1.302 |
| $[Fe(Phen)_3]^{3+/2+}$ | 0.889 | – | 1.155 | *1.277* | 1.370 | 1.322 |
| $[Fe(PyIm_2H_2)_2]^{3+/2+}$ | 0.799 | *0.894* | 1.006 | – | 1.232 | 0.920 |
| $[Fe(Bpteta)]^{3+/2+}$ | 0.619 | – | *0.930* | – | 1.220 | 0.949 |
| $[Fe(tacnPy_2)(AN)]^{3+/2+}$ | 0.926 | *1.091* | 1.229 | – | 1.475 | 1.146 |
| $[Fe(N_4Py)(AN)]^{3+/2+}$ | 0.969 | *1.340* | 1.475 | – | 1.709 | 1.254 |
| $[Fe(Py_3tacn)]^{3+/2+}$ | 0.742 | – | *1.030* | – | 1.278 | 0.974 |
| $[Fe(Pyr_2Py)_2]^{3+/2+}$ | 0.822 | – | 1.140 | – | *1.381* | 1.304 |
| 2+/1+ redox couple | | | | | | |
| $[Fe(PaPy_3)(AN)]^{2+/1+}$ | 0.146 | – | 0.290 | – | *0.402* | 0.452 |
| $[Fe(cyclamAc)(N_3)]^{2+/1+}$ | 1.523 | *1.641* | 1.745 | – | 1.938 | 1.614 |
| $[Fe(N_4Py)Cl]^{2+/1+}$ | 0.731 | *0.834* | 0.903 | – | 1.027 | 0.834 |
| 1+/0 redox couple | | | | | | |
| $[Fe(cyclamAc)(N_3)]^{1+/0}$ | −0.354 | – | −0.261 | – | *−0.196* | −0.126 |
| $[Fe(DITim)_2]^{1+/0}$ | *−0.724* | – | −0.764 | – | −0.785 | −0.438 |
| $[Fe(Pypep)_2]^{1+/0}$ | −0.346 | – | −0.297 | – | *−0.265* | −0.088 |
| $[Fe(PaPy_3)Cl]^{1+/0}$ | *0.055* | – | 0.017 | – | 0.009 | 0.212 |
| $[Fe(PaPy_3)(N_3)]^{1+/0}$ | −0.162 | – | −0.118 | – | *−0.077* | 0.102 |
| $[Fe(PaPy_3)(CN)]^{1+/0}$ | −0.256 | – | −0.093 | – | *−0.014* | 0.232 |
| 1−/2− redox couple | | | | | | |
| $[Fe(SEt)_4]^{1-/2-}$ | *−0.952* | – | −1.056 | – | −1.235 | −0.838 |
| $[Fe(PyIm_2)_2]^{1-/2-}$ | *−0.800* | – | −0.892 | – | −0.990 | −0.460 |
| $[Fe(SCH_2CON(CH_3)_2)_4]^{1-/2-}$ | *−0.505* | – | −0.553 | – | −0.679 | −0.468 |
| $[Fe(S\text{-}i\text{-}Pr)_4]^{1-/2-}$ | *−1.047* | – | −1.152 | – | −1.131 | −0.866 |

In our test sets, there are only three 2+/1+ redox couples. The relatively nonpolar $[Fe(Papy_3)(AN)]^{2+/1+}$ couple is described well using the factor of 1.2. The acetonitrile molecule and the amide group of this complex are included to calculate MA-NPA and the value is 0.485. The performance of the OCV calculation is improved from 0.29 V to 0.402 V, reducing the error from −0.162 to −0.05 V. $[Fe(N_4Py)(Cl)]^{2+/1+}$ and $[Fe(CyclamAc)(N_3)]^{2+/1+}$ couples show the improved results using $f = 1.05$. This modification gives the remarkably refined

OCV results, 0.834 and 1.34 V, respectively, and the corresponding OCV deviation is diminished from 0.069 to 0.000 V and 0.221 to 0.086 V for the two couples. Their MA-NPA are 0.588 and 0.564 which are larger than the value for $[Fe(Papy_3)(AN)]^{1+}$. The chlorine ion of $[Fe(N_4Py)(Cl)]^{1+}$ is included in MA-NPA. In $[Fe(CyclamAc)(N_3)]^{1+}$, the hydrogen atoms attached to the $sp^3$ nitrogen atom, the carboxylate group of CyclamAc ligand, and the $N_3$ ligand contribute to the average of the natural charge. MAE for this group is diminished from 0.121 to 0.026 V. The complexes with MA-NPA smaller than 0.5 are recommend to use $f = 1.2$, and ones with the larger MA-NPA to use smaller cavity of 1.05.

Six couples are in the 1+/0 couple group. The default factor of 1.1 is not so adequate for this group. Three of them require the larger cavity, and two remaining ones need the smaller cavity. The spin state of $[Fe(CyclamAc)(N_3)]^0$ is wrongly predicted and thus excluded from the OCV calculation. One of them requiring the smaller cavity is $[Fe(DITim)_2]^0$ which has large negative charge on the carbon atom of the methyl group near the sulfur donor atom with the average value −0.641. The calculated value −0.724 V is still not satisfactory in comparison to the experimental data −0.438 V. $[Fe(Papy_3)Cl]^0$ also requires the smaller cavity as it has high MA-NPA of 0.691 from the contribution of the chlorine anion and the amide group. For other complexes, $[Fe(Pypep)_2]^0$, $[Fe(PaPy_3)(N_3)]^0$, and $[Fe(PaPy_3)(CN)]^0$ are well described using larger cavity of $f = 1.2$. Their average of natural charge is ranging from 0.552 to 0.575. $[Fe(Pypep)_2]^0$ has 0.573 that is induced from the $sp^3$ nitrogen atom, the hydrogen atom attached to the nitrogen, and the amide group. $[Fe(PaPy_3)(N_3)]^0$, probably due to contributions from the amide group in the $PaPy_3$ ligand and the $N_3$ ligand, has the natural charge 0.539. When the $N_3$ ligand is changed to the CN ligand, MA-NPA is slightly changed to 0.552. For 1+/0 redox couples, the complex with the average charge larger than 0.6 require to use $f = 1.2$. The one with smaller average value is modeled using smaller factor 1.0. The improvement of using optimal scaling factor is quite noticeable, and MAE is reduced to 0.209 V compared with 0.255 V using the default factor.

The last group is the 1−/2− couple. The calculated OCV using the default parameters is quite underestimated. Using default scaling factor yields the error ranging from −0.432 V to −0.085 V with the MAE of 0.255 V, with the largest error −0.432 V occurring for the $[Fe(Pyim_2)_2]^{1-/2-}$ couple. Systems in this group have the large degrees of charge concentration ranging from 0.569 to 0.699. Considering the concentrated charge, the smaller cavity $f = 1.0$ is expected to be optimal and the improvement is noticeable. The disappointing fact, however, is that the $[Fe(Pyim_2)_2]^{1-/2-}$ couple has the quite large error −0.368 V even with the smaller cavity. From the physical argument, atomic radii that make the cavity should not be smaller than vdW radii, and the factor smaller than $f = 1.0$ was not tried. The average error for this group is reduced to −0.168 V. All the predicted OCVs are underestimated, implying systematic errors for which origins are not obvious at the moment.

**Table 5.** The critical charge, different scaling factors, and corresponding MAE depending on the charge state of redox couple.

| | Critical charge (C. C) | Scaling factor | | MAE ( in V ) | |
|---|---|---|---|---|---|
| | | >C. C | <C. C | $F = 1.1$ | $F$ = optimal |
| 3+/2+ | 0.3 | 1.1 | 1.15–1.2 | 0.114 | 0.047 |
| 2+/1+ | 0.5 | 1.05 | 1.2 | 0.121 | 0.026 |
| 1+/0 | 0.6 | 1.0 | 1.2 | 0.255 | 0.209 |
| 1−/2− | All cases need to be described using 1.0 | | | 0.255 | 0.168 |

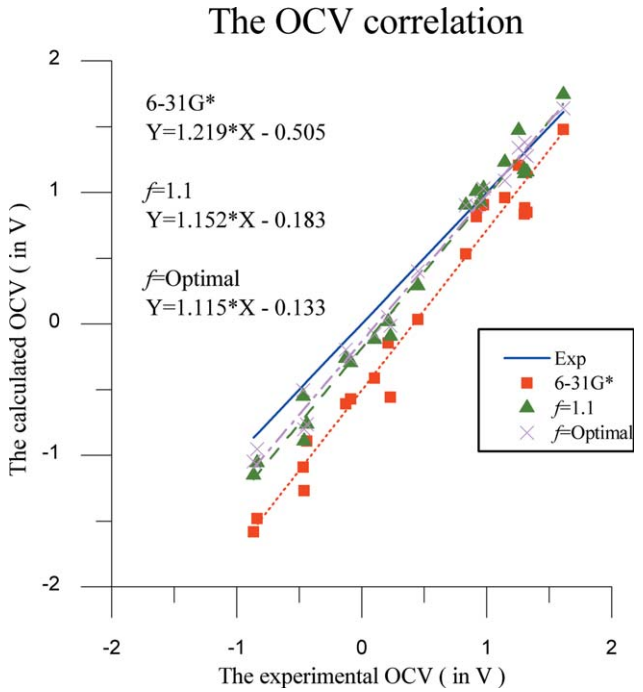


**Figure 3.** The OCV correlation between the experimental and the calculated data. ("6-31G*" is the red, dotted line with square marks. "$f = 1.1$" is the green, dashed line with triangular marks. "$f$ = optimal" is the purple, dash-dotted line with cross marks. The blue line of slope 1 shows perfect correlation between experiment and calculation).

The modified scaling factor according to the MA-NPA value is tabulated in Table 5; the value of the critical charge for each redox couple that can be used to determine the choice of large or small scaling factor is suggested. The complex with larger MA-NPA than the critical charge would be described better using large scaling factor. The different critical charge is chosen depending on the charge of redox couple. The corresponding MAE using $f = 1.1$ and $f$ = optimal are also listed in last two column of Table 5.

Figure 3 shows the correlation between the experimental and the calculated OCV results. The "6-31G*" stands for the calculation using the 6-31G* without any modifications, the "$f = 1.1$" is the calculation using the s6-31G* for the iron atom, the 6-31+G* for the light atoms and the default scaling factor $f = 1.1$. The last "$f$ = Optimal" refers to values obtained by the calculation at the same level as "$f = 1.1$" but using the optimal scaling factor according to the charge state of the

complex. The linear fitting of these data indicates that "$f$ = Optimal" displays the reasonable correlation. The slope of this line is 1.115 which is much closer to unity than other slopes of 1.219 for the "6-31G*" and 1.152 for the "$f$ = 1.1". The y-intercept of −0.505 is severely underestimated in the "6-31G*". The improvements of this part are observed when using spin state corrected basis sets for metal in case of "$f$ = 1.1" and the "$f$ = Optimal" as −0.183 and −0.133, respectively. The promising point is that the "$f$ = Optimal" has a very large $R^2$ value of 0.9902 compared to others. In addition, most of the error occurs in the region of the OCV value lower than 0.2 V. The linear regression for OCVs higher than 0.2 V is $Y$ = 1.001*X+0.015 for "$f$ = Optimal," suggesting the almost perfect correlation. The overall MAE drops to 0.112 V and the mean signed error is −0.088 V, while the MAE of using 6-31G* for whole molecule is 0.408 V and the MAE without the adjustment of scaling factor is 0.188 V. The adjustment of all atomic radii with one scaling factor is a rather crude model, but appears to be quite effective. The use of the different scaling factor for each atom according to its chemical environment is left as the future work.

## Conclusions

One new protocol is developed to estimate OCV of iron complexes reliably using B3LYP and correctly predicted ground spin state. The spin state corrected basis sets on the iron atom and 6-31+G* on ligand atoms can greatly improve the prediction of the ground spin state compared with other B3LYP methods. Considering the volume occupied by the low and high spin state complexes, the inclusion of the cavity creation energy makes the simulation more realistic. With this combination of quantum chemical methods and solvation energy treatment, the correct ground spin state is obtained for all but one of the 21 complexes. The calculation of the accurate OCV is achieved using the different scaling factor for the cavity size according to the partial charges of surface atoms of the complex. The rule of thumb for the optimization is that the larger the MA-NPA, the smaller the scaling factor. The individual atomic charge should, however, be examined together. The MAE of the OCV is remarkably reduced to 0.112 V. The present protocol may be applied to predict OCV of new iron complexes.

## Acknowledgment

The authors thank Dr. Jongtaek Kim for helpful discussion. This work was supported by the Energy Efficiency & Resources of the Korea Institute of Energy Technology Evaluation and Planning (KETEP), and computational resources from KISTI (KSC-2012-C2-42).

**Keywords:** redox potential of iron complexes · redox flow battery · DFT calculation · cavity in solvation model · spin state energy · spin corrected basis set

How to cite this article: H. Kim, J. Park, Y. S. Lee, *J. Comput. Chem.* **2013**, *34*, 2233–2241. DOI: 10.1002/jcc.23380

Additional Supporting Information may be found in the online version of this article.

[1] V. S. Bryantsev, M. S. Diallo, A. C. T. van Duin, W. A. Goddard, III, *J. Phys. Chem. A* **2008**, *112*, 9104.
[2] L. E. Roy, E. Jakubikova, M. G. Guthrie, E. R. Batista, *J. Phys. Chem. A* **2009**, *113*, 6745.
[3] J. Li, C. L. Fisher, J. L. Chen, D. Bashford, L. Noodleman, *Inorg. Chem*, **1996**, *35*, 4694.
[4] M. –H. Baik, R. A. Friesner, *J. Phys. Chem. A* **2002**, *106*, 7407.
[5] R. A. Torres, T. Lovell, L. Noodleman, D. A. Case, *J. Am. Chem. Soc.* **2003**, *125*, 1923.
[6] M. Uudsemaa, T. Tamm, *J. Phys. Chem. A* **2003**, *107*, 9997.
[7] L. Noodleman, T. Lovell, W. -G. Han, J. Li, F. Himo, *Chem. Rev.* **2004**, *104*, 459.
[8] J. P. Holland, J. C. Green, J. R. Dilworth, *Dalton Trans.* **2006**, 783.
[9] J. Moens, G. Roos, P. Jaque, F. De Proft, P. Geerlings, *Chem. Eur. J.* **2007**, *13*, 9331.
[10] J. J. Berard, G. Schreckenbach, P. L. Arnold, D. pater, J. B. Love, *Inorg. Chem.* **2008**, *47*, 11583.
[11] M. T. de Groot, M. T. M. Koper, *Phys. Chem. Chem. Phys*. **2008**, *10*, 1023.
[12] J. Moens, P. Geerlings, G. Roos, *Chem. Eur. J.* **2007**, *13*, 8174.
[13] A. Galstyan, E. Knapp, *J. Comput. Chem.* **2009**, *30*, 203.
[14] S. J. Konezny, M. D. Doherty, O. R. Luca, R. H. Crabtree, G. L. Soloveichik, V. S. Batista, *J. Phys. Chem. C* **2012**, *10*, 116.
[15] T. Matsui, Y. Kitagawa, M. Okumura, Y. Shigeta, S. Sakaki, *J. Comput. Chem.* **2013**, *34*, 21.
[16] T. F. Hughes, R. A. Friesner, *J. Chem. Theory Comput.* **2012**, *8*, 442.
[17] M. Swart, *J. Chem. Theory Comput.* **2008**, *4*, 2057.
[18] M. Swart, A. R. Groenhof, A. W. Ehlers, K. Lammertsma, *J. Phys. Chem. A* **2004**, *108*, 5479.
[19] L. M. L. Daku, A. Vargas, A. Hauser, A. Fouqueau, M. E. Casida, *Chem. Phys. Chem.* **2005**, *6*, 1393.
[20] K. Pierloot, S. Vancoillie, *J. Chem. Phys.* **2006**, *125*, 124303.
[21] O. Salomon, M. Reiher, B. A. Hess, *J. Chem. Phys.* **2002**, *117*, 4729.
[22] M. Reiher, O. Salomon, B. A. Hess, *Theor. Chem. Acc.* **2001**, *107*, 48.
[23] M. Guell, J. M. Luis, M. Sola, M. Swart, *J. Phys. Chem. A* **2008**, *112*, 6384.
[24] M. Swart, M. Guell, J. M. Luis, M. Sola, *J. Phys. Chem. A* **2010**, *114*, 7191.
[25] (a) S. Miertus, E. Scrocco, J. Tomasi, *J. Chem. Phys.* **1981**, *55*, 117; (b) J. Tomasi, M. Persico, *Chem. Rev.* **1994**, *94*, 2027; (c) R. Cammi, J. Tomasi, *J. Comput. Chem.* **1995**, *16*, 1449; (d) E. Cances, B. Mennucci, J. Tomasi, *J. Chem. Phys.* **1997**, *107*, 3032.
[26] K. Kitaura, K. Morokuma, *Int. J. Quantum Chem.* **1976**, *10*, 325.
[27] M. J. Frisch, G. W. Trucks, H. B. Schlegel, G. E. Scuseria, M. A. Robb, J. R. Cheeseman, G. Scalmani, V. Barone, B. Mennucci, G. A. Petersson, H. Nakatsuji, M. Caricato, X. Li, H. P. Hratchian, A. F. Izmaylov, J. Bloino, G. Zheng, J. L. Sonnenberg, M. Hada, M. Ehara, K. Toyota, R. Fukuda, J. Hasegawa, M. Ishida, T. Nakajima, Y. Honda, O. Kitao, H. Nakai, T. Vreven, J. A. Montgomery, Jr., J. E. Peralta, F. Ogliaro, M. Bearpark, J. J. Heyd, E. Brothers, K. N. Kudin, V. N. Staroverov, T. Keith, R. Kobayashi, J. Normand, K. Raghavachari, A. Rendell, J. C. Burant, S. S. Iyengar, J. Tomasi, M. Cossi, N. Rega, J. M. Millam, M. Klene, J. E. Knox, J. B. Cross, V. Bakken, C. Adamo, J. Jaramillo, R. Gomperts, R. E. Stratmann, O. Yazyev, A. J. Austin, R. Cammi, C. Pomelli, J. W. Ochterski, R. L. Martin, K. Morokuma, V. G. Zakrzewski, G. A. Voth, P. Salvador, J. J. Dannenberg, S. Dapprich, A. D. Daniels, O. Farkas, J. B. Foresman, J. V. Ortiz, J. Cioslowski, D. J. Fox, Gaussian 09, Revision B.01; Gaussian, Inc.: Wallingford CT, **2010**.
[28] S. Trasatti, *Pure Appl. Chem.* **1986**, *58*, 955.
[29] C. J. Cramer, D. G. Truhlar, *Phys. Chem. Chem. Phys.* **2009**, *11*, 10757.
[30] S. J. Konezny, M. D. Doherty, O. R. Luca, R. H. Crabtree, G. L. Soloveichik, V. S. Batista, *J. Phys. Chem. C* **2012**, *116*, 6349.
[31] F. J. Luque, M. J. Negre, M. Orozco, *J. Phys. Chem.* **1993**, *97*, 4386.
[32] M. Bachs, F. J. Luque, M. Orozco, *J. Comput. Chem.* **1994**, *15*, 446.

[33] B. Jayaram, R. Fine, K. A. Sharp, B. H. Honig, *J. Phys. Chem.* **1989**, *93*, 4320.
[34] M. Orozco, F. J. Luque, *Chem. Phys.* **1994**, *182*, 237.
[35] M. E. Garcia Posse, M. A. Juri, P. J. Aymonino, O. E. Piro, H. A. Negri, E. E. Castellano, *Inorg. Chem.* **1984**, *23*, 948.
[36] S. Dick, *Z. Kristallogr.-New Cryst. Struct.* **1998**, *213*, 356.
[37] J. L. Pascual-Ahuir, E. Silla, *J. Comput. Chem*. **1990**, *11*,1047.
[38] E. Silla, F. Villar, O. Nilsson, J. L. Pascual-Ahuir, O. Tapia, *J. Mol. Graph.* **1990**, *8*, 168.
[39] E. Silla, I. Tunon, J. L. Pascual-Ahuir, *J. Comput. Chem.* **1991**, *12*, 1077.
[40] M. A. Hoselton, L. J. Wilson, R. S. Drago, *J. Am. Chem. Soc.* **1975**, *97*, 1722.
[41] R. A. Binstead, J. K. Beattie, *Inorg. Chem.* **1986**, *25*, 1481.

Received: 24 January 2013
Revised: 22 June 2013
Accepted: 25 June 2013
Published online on 19 July 2013